Transactions of the Korean Nuclear Society Spring Meeting
Jeju, Korea, May 22-23, 2025

Development of Electrochemical Nickel Coating Technology for Structural Material Protection in Molten Salt Reactor Environments

Younghwan Jeon[a], Jungho Hur[a], Jaeyeong Park[b*]
[a]*Advanced Fuel Cycle Technology Division, Korea Atomic Energy Research Institute,*
111, Daedeok-daero 989beon-gil, Yuseong-gu, Daejeon, 34057, Republic of Korea
[b]*Department of Nuclear Engineering, Ulsan National Institute of Science and Technology,*
50 UNIST-gil, Ulju-gun, Ulsan 44919, Republic of Korea
[*]*Corresponding author: jypark@unist.ac.kr*

Keywords : Nickel, Ni-coating, Molten salt, Molten salt reactor, electrochemistry

1. Introduction

Molten Salt Reactors (MSRs) are a focal point in the development of Generation IV nuclear reactors, leveraging the unique physicochemical attributes of molten salts as both fuel and coolant. These reactors offer inherent safety and economic advantages, stemming from the high boiling points, efficient thermal conductivity, negative temperature coefficients, and inherent radiological stability of molten salts [1, 2]. The pursuit of MSR technology is a global endeavor, with nations like Korea actively engaged in developing chloride-based MSR variants. A significant impediment to the widespread adoption of MSRs is the corrosion of structural materials induced by the molten salt environment.

Molten salt corrosion in MSR systems is a multifaceted phenomenon, driven by electrochemical redox reactions (e.g., $2U^{4+} + Cr \rightarrow 2U^{3+} + Cr^{2+}$), the presence of moisture and oxygen impurities, and chemical interactions with fission products [3, 4]. Conventional mitigation strategies, including electrochemical potential control and the removal of impurities, have demonstrated limited success in completely suppressing corrosion. As an alternative, nickel coatings applied to structural materials have been proposed to enhance corrosion resistance [5].

While pure nickel exhibits superior corrosion resistance in molten salts compared to iron- and nickel-based alloys, its limited mechanical strength and susceptibility to oxidation in air preclude its direct use as a structural material [6, 7]. Consequently, the application of nickel coatings to structural alloys, specifically on surfaces in contact with the molten salt, is hypothesized to provide a synergistic combination of mechanical integrity and corrosion protection. Preliminary investigations have shown that nickel coatings can effectively enhance corrosion resistance, but localized and aggressive corrosion, characterized by pitting and crevice formation, has been observed at defect sites within the coating. Furthermore, concerns regarding the long-term durability of the nickel coating have been raised due to alloying effects.

This study aims to address these challenges through the development of an electrochemical nickel coating technology tailored for molten salt systems. The Periodic Pulse Reverse Plating (PPRP) technique was employed to fabricate dense and uniform nickel coatings on a 90Ni–10Mo alloy, a surrogate for nickel-based structural materials, within a $NaCl–MgCl_2–NiCl_2$ molten salt electrolyte at 700 ℃. The PPRP process parameters were optimized to facilitate the restoration of micro-cracks in the alloy substrate. Additionally, the efficacy of the nickel coating technique was evaluated in molten salt systems simulating the presence of fission products ($NaCl–MgCl_2–NiCl_2–NdCl_3$) and fuel components ($NaCl–MgCl_2–NiCl_2–EuCl_3$).

2. Experimental procedure

2.1 Electrochemical cell

All electrochemical experiments and salt preparation procedures were conducted within a controlled atmosphere glovebox, maintaining moisture and oxygen levels below 0.1 ppm. Reagent-grade NaCl (Alfa Aesar, 99.99%) and $MgCl_2$ (Alfa Aesar, 99.99%) were subjected to a multi-step preheating protocol at 200 ℃, 400 ℃, and 600 ℃ for 24 hours each, followed by purging with gaseous CCl_4 in an Ar carrier at 600 ℃ for 4 hours to minimize residual moisture and oxygen.

The electrochemical properties of Ni^{2+} ions in the $NaCl–MgCl_2$ molten salt were investigated using cyclic voltammetry (CV). The concentration of $NiCl_2$ in the $NaCl–MgCl_2$ electrolyte ranged from 0.1 to 1.0 wt%, and the scan rate varied from 50 to 1000 mV s^{-1}. As depicted in Fig. 1 (a), a thin quartz tube containing $NaCl–MgCl_2–1$ wt% AgCl served as the reference electrode, while a 1.0 mm diameter tungsten wire and a 4.0 mm diameter tungsten rod were used as the working and counter electrodes, respectively.

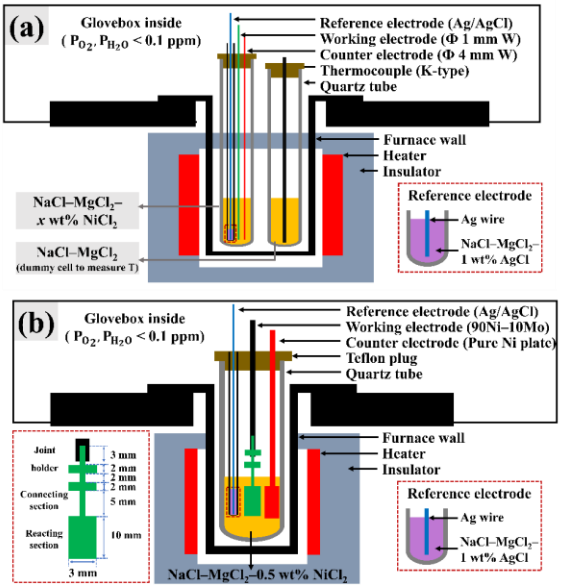

Fig. 1. Schematics of an electrochemical cell for the electrochemical property measurement experiment (a) and the Ni-coating experiment (b)

To evaluate the nickel coating technology in the molten salt system, a 90Ni–10Mo alloy was selected as a surrogate for nickel-based alloys used in MSRs. Molybdenum (Mo) was chosen as an alloying element due to its more positive redox potential compared to nickel, precluding its electrochemical reaction during nickel deposition. Furthermore, the low concentration of Mo facilitates the differentiation of the coated region using SEM–EDS techniques, including variations in secondary electron (SE) image contrast, elemental mapping, and quantitative composition analysis.

Specimens of the 90Ni–10Mo alloy, with a thickness of 2 mm, were fabricated into the geometry shown in Fig. 1 (b). The exposed surface area was 100 mm^2, and the specimens were polished to a 2000-grit finish prior to experimentation. Select specimens were subjected to focused ion beam (FIB) milling to create two micro-cracks, each with dimensions of 500 μm × 3 μm × 7 μm, to assess the efficacy of the electrochemical technique in repairing surface defects. The 90Ni–10Mo specimen, attached to a thin tungsten wire and secured within a quartz guide tube, served as the working electrode. A pure nickel plate (Goodfellow, >99.0 wt%), also attached to a tungsten wire, was employed as the counter electrode. Each experiment utilized 15.000 g of NaCl–$MgCl_2$–0.5 wt% $NiCl_2$ with or without 0.5 wt% $NdCl_3$ or $EuCl_3$.

2.2 Periodic Pulse Reverse Plating (PPRP)

The deposition of nickel under constant cathodic potential or current density in the molten salt system typically results in the formation of dendritic structures (Fig. 2 (a)). The PPRP method, as illustrated in Fig. 2 (b), mitigates this issue by alternating between cathodic and anodic conditions. During the cathodic phase, nickel dendrites are formed, while the subsequent anodic phase selectively dissolves the edges of these dendrites. By repeating this cycle, a smooth and dense nickel coating is expected to form.

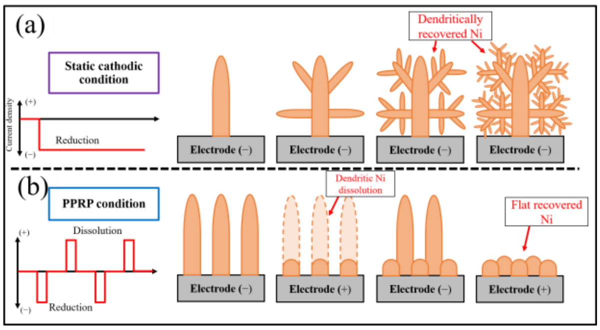

Fig. 2. Schematics of the reduced Ni products; static cathodic condition (a) and PPRP condition (b)

3. Results

3.1 Electrochemical properties of the Ni^{2+} ion in molten NaCl–$MgCl_2$

The electrochemical behavior of Ni^{2+} ions in the molten NaCl–$MgCl_2$ electrolyte was characterized using CV. Analysis of the cathodic peak data and half-peak potentials derived from the CV curves allowed for the determination of the diffusion coefficient and formal potential of Ni^{2+}. For the reversible soluble–insoluble reaction, the diffusion coefficient was calculated using the Berzins-Delahay equation (Equation 1):

$$(1)\quad j_p = 0.6105\, C_O^{*} nF \sqrt{\frac{nFDv}{RT}}$$

The calculated diffusion coefficient for Ni^{2+} ions in the 700 °C NaCl–$MgCl_2$ melt was 2.88×10^{-5} cm^2 s^{-1}, with a standard deviation of 0.150×10^{-5} cm^2 s^{-1}.

The formal potential ($E^{0'}$) was determined using the Tylka equation (Equation 2):

$$(2)\quad E_{1/2} = E^{0'} + \frac{RT}{nF}\ln\left(\frac{C_O^{*}}{2C^{0}}\right)$$

The calculated formal potential in the NaCl–$MgCl_2$–0.5 wt% $NiCl_2$ melt was found to be 0.26 V (vs. 1 wt% Ag/AgCl).

3.2 Ni-coating technology verification through PPRP method

Preliminary experiments were conducted under various PPRP conditions to optimize the nickel coating process. A uniform nickel coating was obtained using cathodic and anodic conditions of −6 and +4 mA cm^{-2}, respectively, with a 0.8-second rest time (Fig. 3).

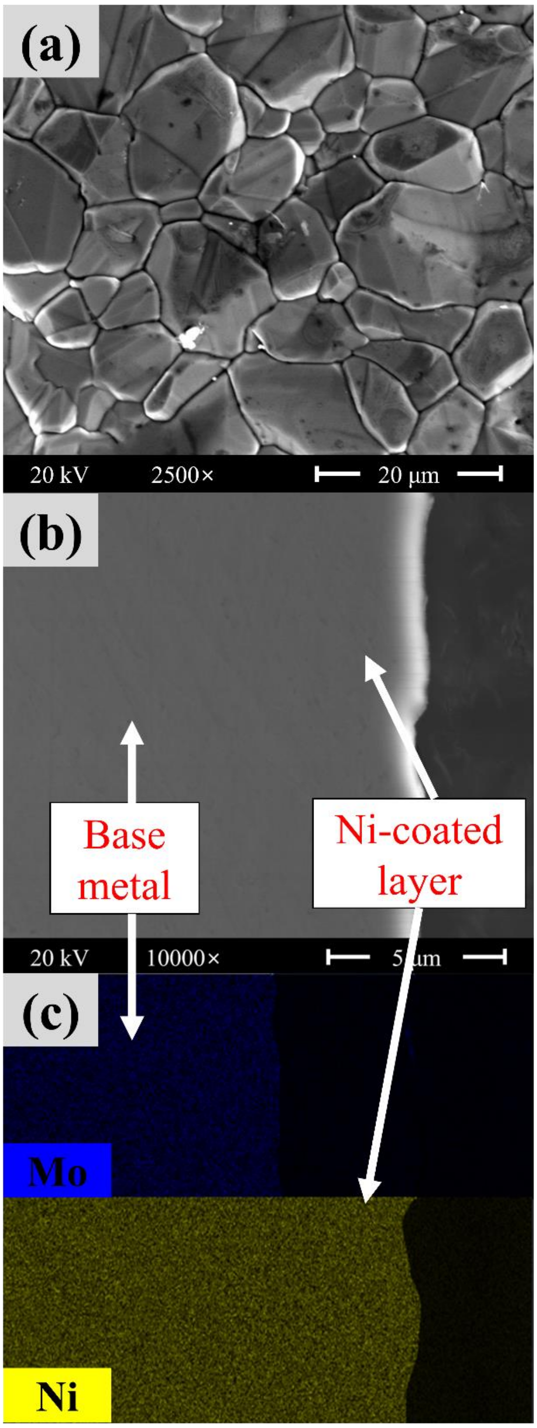

Fig. 3. SEM–EDS images of the Ni-coated 90Ni–10Mo alloy (a; surface, b; cross-section, and c; EDS mapping)

Increasing the difference between the cathodic and anodic conditions (−30/+20, −60/+40 mA cm^{-2}) resulted in imperfect nickel coatings (Fig. 4). Notably, increasing the applied current density led to the formation of voids between the base metal and the nickel coating (Fig. 4 (c, d)).

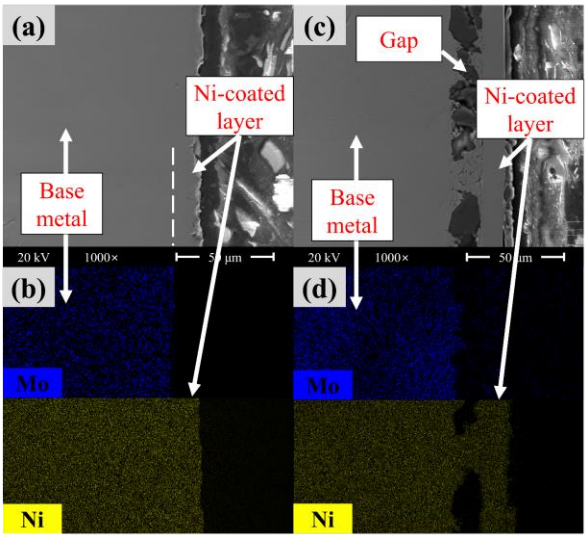

Fig. 4. SEM–EDS images of the Ni-coated layer with harsh current density condition

The application of electrochemical potentials is crucial for controlling the desired reaction in an actual MSR system. Appropriate nickel coatings were formed under moderate potential conditions (Fig. 5 (a, b)). However, increasing the potential gap resulted in porous nickel layers (Fig. 5 (c–f)).

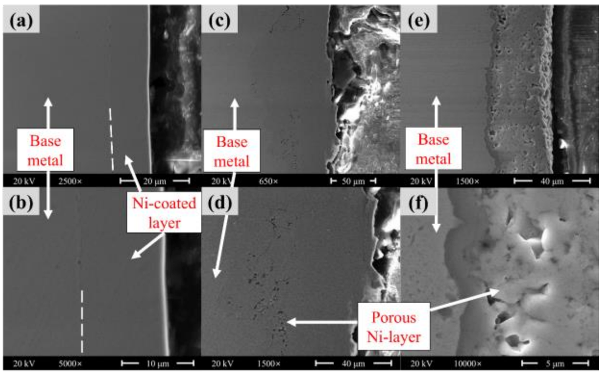

Fig. 5. SEM–EDS images of the Ni-coated layer with different applied potential conditions

The restoration of micro-cracks that expose the structural material to the molten salt is essential for mitigating corrosion. By applying moderate redox conditions, micro-cracks with a width of 3 µm were filled with nickel (Fig. 6 (a–c, g–i)). Conversely, less controlled conditions resulted in the nickel coating simply covering the cracks without complete restoration (Fig. 6 (d–f)).

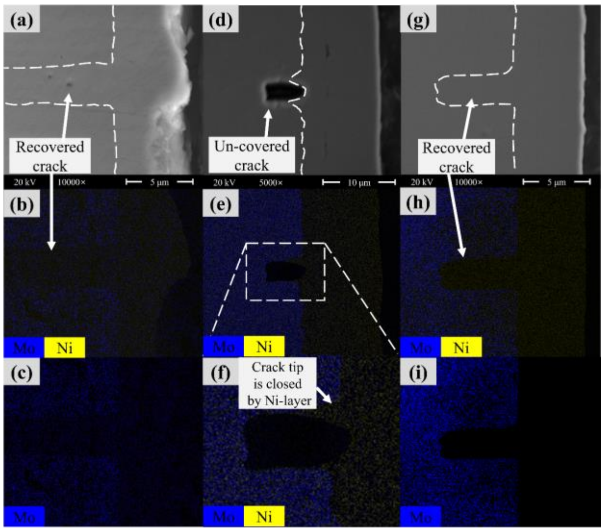

Fig. 6. SEM–EDS images of the restored crack with PPRP technique with different conditions

4. Discussion

The quality of the nickel coating layer is intricately linked to the interplay between the applied current density, cathodic potential, rest time, and electrolyte composition. In general, the use of moderate redox conditions coupled with an adequate rest time yields high-quality nickel coatings, while immoderate redox conditions in conjunction with a short rest time yield lower-quality coatings. The PPRP method relies on the effective dissolution of dendritic nickel formations during the anodic phase. This results in layered nickel deposition and increases the net amount of recovered nickel per unit process. Insufficient diffusion of Ni^{2+} ions to the nickel layer surface during the rest time can also lead to the formation of porous nickel layers as recovery preferentially progresses at the tips of the nickel layer surface.

In an operational MSR system, the molten salt electrolyte will contain a variety of dissolved ionic species, including fissile materials, fission products, and alloying elements. In this study, the presence of $NdCl_3$, a surrogate for fission products, did not impede nickel coating using the PPRP method, owing to the more negative redox potential of Nd^{3+} compared to Ni^{2+}. However, Ni-coating via PPRP was significantly hindered in the presence of $EuCl_3$, used to simulate fissile elements. The more positive redox potential of the Eu^{3+}/Eu^{2+} couple compared to Ni^{2+} resulted in continuous electrochemical reactions involving Eu^{3+} ions during the PPRP process. The reaction between Eu^{3+} and Ni ($2Eu^{3+} + Ni \rightarrow 2Eu^{2+} + Ni^{2+}$) necessitates the meticulous control of process parameters, including applied redox conditions and rest time, to achieve effective nickel deposition.

5. Conclusion

This study investigated the electrochemical nickel coating technology for molten salt systems. The effects of varying process parameters on the quality of the nickel coating layer were evaluated, and the potential for micro-crack restoration was demonstrated. The feasibility of applying nickel coatings in simulated MSR electrolytes containing fission products ($NdCl_3$) and fissile elements ($EuCl_3$) was also assessed. The results of this study have implications for a variety of industries beyond the nuclear sector.

Acknowledgment

This work was supported by the Molten Salt Reactor Development Agency grant funded by the Korea government (the Ministry of Science and ICT) [Project Number: RS-2023-00261146]

REFERENCES

[1] R. Roper, M. Harkema, P. Sabharwall, C. Riddle, B. Chisholm, B. Day, P. Marotta, Molten salt for advanced energy applications: A review, Annals of Nuclear Energy, Vol. 169, p. 108924, 2022.
[2] L. Chen, L.-Y. He, B. Zhou, G.-F. Zhu, Y.-H. Fan, H.-J. Xu, R. Yan, Y. Zou, Evaluation on 131I production based on molten salt reactor off-gas extraction, Annals of Nuclear Energy, Vol. 195, p. 110192, 2024.
[3] J. Zhang, C.W. Forsberg, M.F. Simpson, S. Guo, S.T. Lam, R.O. Scarlat, F. Carotti, K.J. Chan, P.M. Singh, W. Doniger, Redox potential control in molten salt systems for corrosion mitigation, Corrosion Science, Vol. 144, pp. 44-53, 2018.
[4] V. Afonichkin, A. Bovet, V. Shishkin, Salts purification and voltammetric study of the electroreduction of U (IV) to U (III) in molten LiF–ThF4, Journal of nuclear materials, Vol. 419, pp. 347-352, 2011.
[5] O. Beneš, E. Capelli, N. Morelová, J.-Y. Colle, A. Tosolin, T. Wiss, B. Cremer, R. Konings, Cesium and iodine release from fluoride-based molten salt reactor fuel, Physical Chemistry Chemical Physics, Vol. 23, pp. 9512-9523, 2021.
[6] H. Jin, Y.-Y. Wang, Y.-T. Wang, H.-B. Yang, Synthesis and properties of electrodeposited Ni–CeO 2 nano-composite coatings, Rare Metals, Vol. 37, pp. 148-153, 2018.
[7] A. Rashidi, A. Amadeh, Effect of electroplating parameters on microstructure of nanocrystalline nickel coatings, Journal of Materials Science & Technology, Vol. 26, pp. 82-86, 2010.